

# Probing Hybridization parameters from microarray experiments: nearest neighbor model and beyond

W.W. Hadiwikarta<sup>1,2</sup>, J.-C. Walter<sup>2</sup>, J. Hooyberghs<sup>1,3</sup>, E. Carlon<sup>2,1,\*</sup>

<sup>1</sup>*Flemish Institute for Technological Research, VITO, Boeretang 200, B-2400 Mol, Belgium*, <sup>2</sup>*Institute for Theoretical Physics, KULeuven, Celestijnenlaan 200D, B-3001 Leuven, Belgium*,  
and <sup>3</sup>*Department WNI, Hasselt University, Campus Diepenbeek, Agoralaan - Building D, B-3590, Diepenbeek, Belgium*

In this article it is shown how optimized and dedicated microarray experiments can be used to study the thermodynamics of DNA hybridization for a large number of different conformations in a highly parallel fashion. In particular, free energy penalties for mismatches are obtained in two independent ways and are shown to be correlated with values from melting experiments in solution reported in the literature. The additivity principle, which is at the basis of the nearest-neighbor model, and according to which the penalty for two isolated mismatches is equal to the sum of the independent penalties, is thoroughly tested. Additivity is shown to break down for a mismatch distance below 5 nt. The behavior of mismatches in the vicinity of the helix edges, and the behavior of tandem mismatches are also investigated. Finally, some thermodynamic outlying sequences are observed and highlighted. These sequences contain combinations of GA mismatches. The analysis of the microarray data reported in this article provides new insights on the DNA hybridization parameters and can help to increase the accuracy of hybridization-based technologies.

## I. INTRODUCTION

Hybridization of single-stranded nucleic acids to form a duplex is a reversible chemical reaction, which is at the basis of many processes and techniques currently used in biotechnology, as for instance PCR [1]. Due to its central importance, hybridization has been intensively studied in experiments (focusing on the thermodynamics [2, 3] or kinetics of the process) and also in computer simulations [4].

The thermodynamics of DNA hybridization is usually described by the nearest-neighbor (NN) model [5]. This model assumes that the free energy of a duplex can be expressed as a sum of dinucleotide stability parameters; it is therefore based on the principle of additivity. From the NN parameters one can, for instance, estimate melting temperatures, compute melting curves and predict secondary structures in which RNA molecules fold [6, 7]. In the folding problem, many different local conformations arise as single nucleotide mismatches, bulges, stem-loop structures, etc. Describing these conformations in the framework of the NN model is very challenging and requires a large number of parameters [6]. However, only a limited number of them have been measured directly in experiments [8]. In addition, one may also wonder whether additivity holds in such cases. To investigate a large number of different conformations, it would be very advantageous to have access to high-throughput mea-

surements, provided that they are sufficiently accurate.

In this article, we quantitatively determine free energy penalties for mismatches using microarray data obtained from a set of optimized and dedicated experiments. In DNA microarrays, several thousand of different sequences can be spotted at a surface, hence a large number of hybridization reactions takes place simultaneously. We use two different approaches: the first one is based on a linear regression of a large set of experimental data points ( $\approx 1000$ ) to fit 58 NN dinucleotide parameters. The second method relies on the computation of the logarithm of the ratios of fluorescent intensities measured from different spots of the arrays. We show that both methods provide highly correlated set of NN parameters. In addition, the second approach allows to probe the limitations of the NN model. It is found that when two mismatches are closer than 5 nt additivity breaks down and the free energy of the duplex is not equal to the sum of the two separate contributions of isolated mismatches. We also quantify the influence of mismatches close to the edge of the double helix and show that the free energy penalty is much weaker in those cases. Overall, this work provides new insights on DNA hybridization thermodynamics and can help to increase the accuracy of hybridization-based technologies.

## II. MATERIALS AND METHODS

The experiments were performed on custom Agilent arrays, following a standard protocol, which is discussed in [9]. In each experiment, a single target sequence in solution was hybridized at concentrations ranging typically from  $\sim 10$  picoM to  $\sim 2$  nanoM. In total, three

---

\* To whom correspondence should be addressed:  
Tel: +32 16 32 72 39  
Fax: +32 16 32 79 86  
Email: enrico.carlon@fys.kuleuven.be

$t_1$ : 5'-CTGGTCTTAGATGC <b>AGC</b> GACTGTT-poly(A)-3'-Cy3
$t_2$ : 5'-CTGCACAATTCCG <b>GAG</b> CTATGAATT-poly(A)-3'-Cy3
$t_3$ : 5'-AATAATGCTCATTAGGCACCGGAA-poly(A)-3'-Cy3

TABLE I. Target sequences used in the experiments. At the 3' side of each sequence a 20-mer poly(A) is attached, terminating with a Cy3 fluorophore. The targets were selected from Optimal Design criteria [2] (Supplementary Data). Each target is hybridized separately on specific microarrays containing mismatched probes with up to two mismatches with respect to the target. Note that  $t_1$  and  $t_2$  share a common triplet of nucleotides AGC at the same sequence position (in bold characters). The mismatches centered around this triplet will be discussed in some details in the 'Results' section.

different sets of experiments were performed using the target sequences shown in Table I. These sequences were selected from 25-mers human DNAs using Optimal Design methods [2]. The theory of Optimal Design provides some criteria of selecting an optimal set of measurements, which minimize the uncertainties in the parameters of a statistical model (see Supplementary Data).

From the targets of Table I, three different microarrays were designed and used for hybridization to either  $t_1$ ,  $t_2$  or  $t_3$ . Each microarray contains probes with either zero, one or two mismatches with respect to the given target, covering all possible mismatch combinations. In a stretch of  $N$  nucleotides there can be  $3N$  single mismatch probes and  $9N(N-1)/2$  double mismatch probes. For  $N = 25$  this gives in total 2776 different sequences, which were spotted in the microarray. The sequences were replicated 15 times to fill up completely a 44K custom Agilent array. Another design was also used mismatches have a minimal distance of 4 nt from the border and a minimal relative distance of 5 nt. In this case the total number of sequences is 646. These sequences were replicated 23 times to fill a 15K custom arrays. We considered hybridizing sequences of 25 nucleotides. This is because in previous studies [11] these sequences were found to attain thermodynamic equilibrium after  $\sim 3$  h of hybridization (in the experiments the hybridization time is of 17 h, hence thermodynamic equilibrium is guaranteed). A hybridization experiment provides a large number of fluorescence intensities: the highest intensity is from spots containing perfect match sequence, whereas the intensity decreases with the number and type of mismatches. The reduction of the intensity provides an estimate of the hybridization free energy. We use two different methods to obtain the NN parameters, as discussed in the next sections.

### III. RESULTS

#### A. Nearest-neighbor parameters from linear regression

Equilibrium thermodynamics predicts that the measured fluorescence intensity from a spot  $i$  equals to:

$$I_i = I_0 + Ace^{-\Delta G_i/RT} \quad (1)$$

where  $\Delta G_i$  is the hybridization free energy between the target sequence and a probe sequence in  $i$ ,  $A$  is a pa-

rameter, which sets the intensity scale,  $c$  the target concentration,  $R$  the gas constant and  $T$  the temperature (experiments are performed at  $T = 65^\circ\text{C} = 338\text{K}$ , which is the value of the temperature used in the rest of the analysis). Although the data analyzed are background-subtracted from the Agilent scanner, there remains always some small aspecific signals, which we denote by  $I_0$  in Equation (1). In the experiments  $I_i$  is obtained from the average over typically approximately 15 replicated spots. One should note that Equation (1) is valid at sufficiently low target concentrations, i.e. when only a limited fraction of probes is hybridized in a spot, hence far from chemical saturation. On the other hand, at very low concentrations, the specific signal, i.e. the second term in Equation (1), can become comparable to  $I_0$ . Therefore, for the analysis of the data we restricted ourselves to intermediate concentrations and intensities for which we explicitly verified that the intensities scale linearly with concentrations, as predicted by Equation (1) (more details can be found in the Supplementary Data). In the intensity scale of the experiments  $I_0 \approx 1$ , whereas the values used in the analysis are  $I_i \gtrsim 10$ . In practice, the large majority of the intensities in experiments with target concentration  $c = 100$  pM or higher are above this threshold value.

In the following, we will consider the logarithm of the intensities measured with respect to the perfect match (PM) intensity. Using Equation (1), for  $I_i \gg I_0$  we get:

$$y_i \equiv \ln I_i - \ln I_{PM} = -\frac{\Delta G_i - \Delta G_{PM}}{RT} \quad (2)$$

which defines the free energy penalty of probe  $i$  with respect to the perfectly matching probe. This penalty can be expressed as a sum of NN dinucleotide parameters. Consider, for instance, the example of a probe  $i$  with a single mismatch of type A with respect to the target nucleotide G and with neighboring nucleotides G and T. We have:

$$\begin{aligned} \Delta G_i \left( \begin{array}{c} \dots G \underline{A} T \dots \\ \dots C \underline{G} A \dots \end{array} \right) - \Delta G_{PM} \left( \begin{array}{c} \dots G C T \dots \\ \dots C G A \dots \end{array} \right) = \\ \Delta G \left( \begin{array}{c} G \underline{A} \\ C \underline{G} \end{array} \right) + \Delta G \left( \begin{array}{c} \underline{A} T \\ \underline{G} A \end{array} \right) \\ - \Delta G \left( \begin{array}{c} G C \\ C G \end{array} \right) - \Delta G \left( \begin{array}{c} C T \\ G A \end{array} \right) \\ \equiv \Delta \Delta G \left( \begin{array}{c} G \underline{A} T \\ C \underline{G} A \end{array} \right) \end{aligned} \quad (3)$$



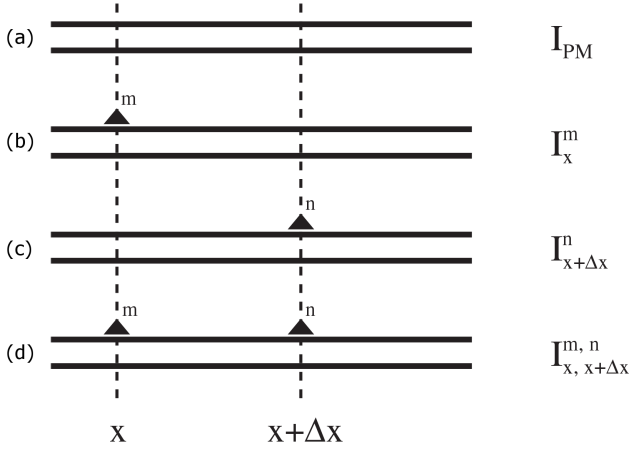


FIG. 3. Schematic representation of hybridizing strands in the microarray experiment. From the appropriate ratios of intensities measured from these spots, the free energy parameters can be determined and the additivity principle can be tested. As in the rest of the article the lower strand is the fixed target sequence. The upper strand is the probe sequence. The filled triangles denote mismatching nucleotides. In the four examples from the top we show: (a) hybridization with a PM probe, (b,c) hybridization with a single mismatch probe where the mismatching nucleotides are  $m$  and  $n$  at positions  $x$  and  $x + \Delta x$  respectively, (d) hybridization with a probe carrying two mismatches. We use the notations  $I_x^m$ ,  $I_{x+\Delta x}^n$  and  $I_{x,x+\Delta x}^{m,n}$  to denote the corresponding intensities measured in the experiment.

### B. Nearest-neighbor parameters from ratios of intensities: probing additivity

The crucial assumption of the NN model is additivity of local free energy contributions. We probe here the limits of additivity of free energy penalties as a function of the distance between two mismatches. We will access the free energy parameters by comparing ratios of intensities measured from different spots in the microarray.

Hereto, we combine microarray spots that contain probes with zero, one or two mismatches with respect to the target and we denote the location of the mismatch by  $x$  or  $x + \Delta x$  as illustrated in Figure 3. The associated free energy penalties can then be derived from the intensity measurements as follows

$$\Delta\Delta G_x^m = -RT \ln \left( \frac{I_x^m}{I_{PM}} \right) \quad (4)$$

$$\Delta\Delta G_{x+\Delta x}^n = -RT \ln \left( \frac{I_{x+\Delta x}^n}{I_{PM}} \right) \quad (5)$$

$$\Delta\Delta G_{x,x+\Delta x}^{m,n} = -RT \ln \left( \frac{I_{x,x+\Delta x}^{m,n}}{I_{PM}} \right) \quad (6)$$

in which the superscript  $m$  and  $n$  represent the three possible mismatching nucleotides at location  $x$  and  $x + \Delta x$  respectively. If the additivity of the NN model holds, the free energy penalty of Equation (6) should equal the

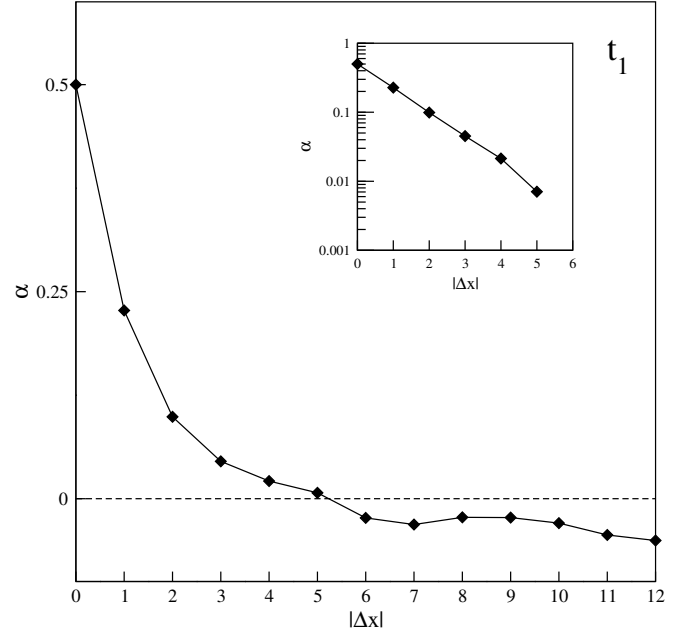


FIG. 4. Parameter  $\alpha$ , the relative deviation from additivity, from the experiment of target  $t_1$ , averaged over  $x, m$  and  $n$  as a function of the distance  $|\Delta x|$  between two mismatches. The inset shows the plot with  $\alpha$  in log scale.

sum of the individual penalties of Equations (4) and (5). To test this, we introduce

$$\alpha = \frac{\Delta\Delta G_x^m + \Delta\Delta G_{x+\Delta x}^n - \Delta\Delta G_{x,x+\Delta x}^{m,n}}{\Delta\Delta G_x^m + \Delta\Delta G_{x+\Delta x}^n} \quad (7)$$

which measures the relative deviation from additivity. Figure 4 shows the experimental results for  $\alpha$  in which we averaged over  $x, m$  and  $n$ , leaving  $\alpha$  as a function of the distance  $|\Delta x|$  between two mismatches. From this data, we notice that  $\alpha$  has a value of about zero when the mismatches are separated by  $\geq 5$  nt, but a clear positive value for smaller  $\Delta x$ . Apparently the free energy penalty of two nearby mismatches is smaller than the sum of the two individual contributions, resulting in a positive  $\alpha$ . Furthermore, the inset from Figure 4 shows that the relationship is linear in a semi logarithmic plot, hence  $\alpha$  decays exponentially with  $|\Delta x|$ . Note that at  $\Delta x = 0$  only one mismatch is present, hence  $m = n$  and  $\alpha$  will be identical to  $1/2$  according to Equation (7). All these observation result from direct measurement values, containing no fitting parameters and strongly suggest that in double-stranded DNA, mismatches have a physical interaction with each other which decays exponentially to zero over a distance of about five nucleotides.

These results are setting some limitations on the additivity of the NN model. However, outside this interaction region of 4 nt we expect the NN model to hold i.e.  $\alpha$  should be zero and mismatches can be considered as isolated. This can be explicitly checked in a very direct

way. When  $\alpha = 0$  we get from Equation (7)

$$\Delta\Delta G_x^m = \Delta\Delta G_{x,x+\Delta x}^{m,n} - \Delta\Delta G_{x+\Delta x}^n. \quad (8)$$

The free energy penalty  $\Delta\Delta G_x^m$  of a mismatch  $m$  at location  $x$ , which we will call the focus mismatch  $(m, x)$ , can be estimated either directly using Equation (4) or via a second mismatch  $(n, x + \Delta x)$  using Equations (5) and (6) for any choice of  $n$  and  $\Delta x > 4$ . Hence, the free energy penalty of the focus mismatch can be estimated from measurements in many independent ways and they should provide the same answer if additivity holds. Note that, using Equations (5) and (6)  $I_{PM}$  drops out in the right hand side of Equation (8).

Figure 5 illustrates how Equation (8) can be used to estimate the  $\Delta\Delta G$  using different combinations of  $n$  and  $\Delta x$ . In this specific example we consider  $\Delta\Delta G_{10}^A$  which corresponds both for target  $t_1$  and  $t_2$  to  $\Delta\Delta G \begin{pmatrix} GAT \\ CGA \end{pmatrix}$  (in the Supplementary Data, we show other examples featuring additivity for different focus mismatches).

In the pane for target  $t_2$ , all the estimates of the free energy penalty are close to each other, the  $48 + 1$  estimates tightly lie around a median value, in this case  $\sim 2.1$  kcal/mol, indicated by the dotted line. The picture in the right pane is a typical one which we observe for any focus mismatch  $(m, x)$ . This confirms that additivity holds in the regime  $\Delta x > 4$ , i.e. when mismatches are separated by  $> 4$  nt. Moreover, it shows that the microarray measurement is internally consistent. Secondly, the left pane, i.e. experiment  $t_1$ , provides the same median value for the free energy penalty, showing also the robustness of the microarray approach to estimate free energies of DNA structures. However, this figure was chosen because it is atypical in the sense that one notices two pronounced outlying values. They correspond to a sequence where both the focus mismatch and the second mismatch are of type  $AG$ . Since they clearly deviate from an otherwise nicely consistent picture, we believe there must be a physically underlying reason for it. We will come back to this point in the section where we discuss thermodynamic outliers.

Note that with this second method we accessed values for the free energy penalties of isolated mismatches without using any multiple regression or fitting procedure, but we simply compared the ratios of intensities, Equations (4)-(6), to get a consistent set of independent estimates. The free energy penalties are then obtained from the median over all data points. We compared the free energy penalties obtained from this method (median) with those obtained from linear regression as discussed in the previous section. The two sets of data are well-correlated with a Pearson correlation coefficient equal to 0.966 (see Supplementary Data). This correlation shows the equivalence of the two approaches. In this analysis, we restricted ourselves to mismatches in the bulk of the sequence, i.e.  $x$  is  $> 5$  nt from the border. Closer to the border we observe boundary effects, which are covered in the next section.

### C. Boundary effects

The previous section ended by showing the equivalence of both approaches to access free energy penalties of an isolated mismatch, provided the data are restricted to bulk mismatches. The direct median method of the previous section can also assess penalties of mismatches close to the boundary, whereas on the contrary the fitting method cannot by construction. The latter, however, has the advantage of fitting a full parameter set of the NN model and as such can easily provide bulk values for the free energy penalty of any isolated mismatch. The combination of both methods now provides an elegant way to assess the effect of boundary proximity on an isolated mismatch. Hereto, we introduce the parameter  $\beta$  as the relative reduction of free energy penalty of a mismatch when compared to its bulk value.

$$\beta = \frac{\Delta\Delta G_x^m}{\Delta\Delta G_{bulk}^m} \quad (9)$$

In Figure 6 the parameter  $\beta$  is shown as a function of  $x$  after averaging over  $m$ . It is clear that, as expected,  $\beta$  is approximately equal to one in the bulk, whereas when approaching the boundary, a reduction of free energy penalty occurs which reaches up to 80%. Note that for mismatches at the boundary,  $x = 1$  and  $x = 25$ , the NN model is not applicable and no data is presented. Figure 6 shows that the range of the boundary effect is  $\sim 4$  nt.

### D. Thermodynamic outliers

As a final result of this article, we come back to the two outliers observed in Figure 5(a); the same deviations are found in replicated experiments at different concentrations: therefore, they are unlikely due to experimental errors. For these two cases we find  $\Delta\Delta G_{10,15}^{A,G} - \Delta\Delta G_{15}^G \approx 1.2$  kcal/mol and  $\Delta\Delta G_{10,17}^{A,G} - \Delta\Delta G_{17}^G \approx 3.1$  kcal/mol, strongly deviating from the median value ( $\approx 2.1$  kcal/mol). The common feature of these two sequences is that they involve GA mismatches. The two sets of mismatches are arranged in an antiparallel way i.e. one G and one A are on the same strand. Mismatches of GA type in DNA and RNA helices have been the subject of several studies in the past [14–21]. In the RNA folding, it is known that GA pairs contribute substantially to the RNA helix stability. Their contribution is comparable to that of a canonical AT pair. As AT pairs, GA form two hydrogen bonds, but can also assume four different conformations [14]. The microarray data suggest that the antiparallel combination of GA and AG pairs of mismatches have a long range interaction effect, which is probably a signature of some structural conformational change of a double helix containing these pairs. Next-nearest neighbor effects extending up to 4 nt distance for antiparallel GA mismatches have been reported in the

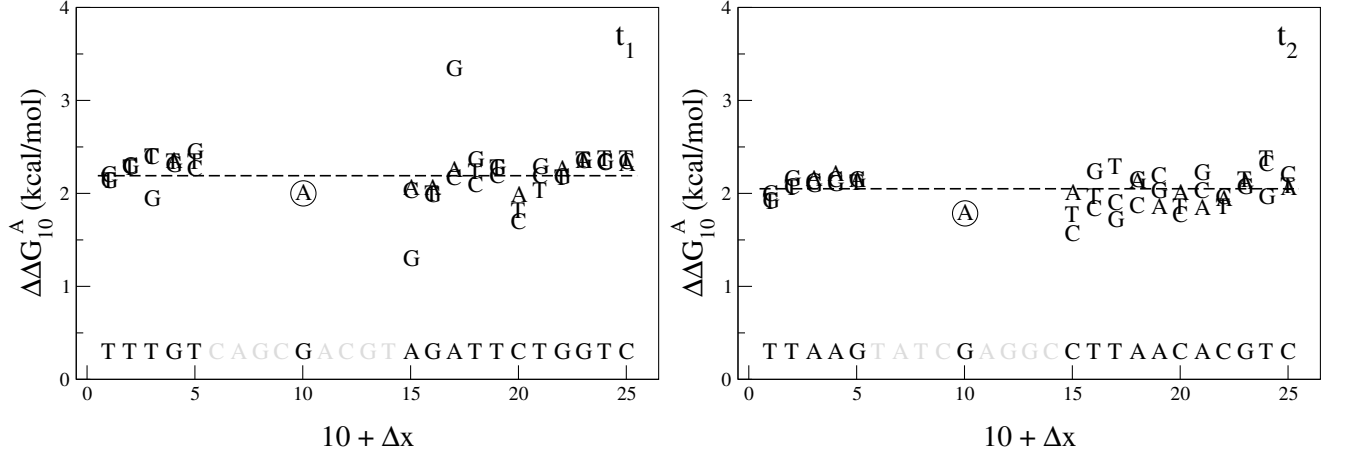


FIG. 5. Free energy penalty  $\Delta\Delta G_{10}^A$  for focus mismatch ( $m = A, x = 10$ ) derived from experimental intensities according to Equation (8) as a function of the location  $x + \Delta x$  of the second mismatch ( $n, x + \Delta x$ ). For each  $|\Delta x| > 4$  the three values, one per possible mismatch, are indicated by the letter representing the mismatching nucleotide  $n$  of the probe. The target sequence is written in top of the x-axis in 3'-5' notation,  $t_1$  in left pane,  $t_2$  in right pane. The dotted line corresponds to the median value of the 48 estimates. The circled point is the estimate without second mismatch coming from Equation (4). For this particular mismatch, the free energy penalty for both  $t_1$  and  $t_2$  is identical and corresponds to  $\Delta\Delta G \left( \frac{GAT}{CGA} \right)$ .

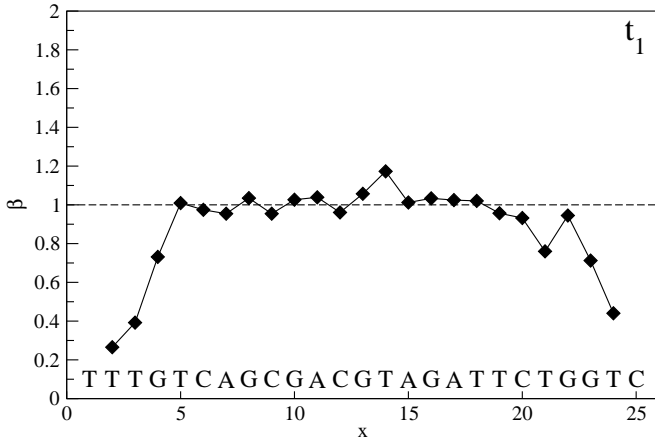


FIG. 6. Boundary effect:  $\beta$ , the relative reduction of mismatch free energy penalty, as a function of location for experiment with target  $t_1$ . Each point is the average of three estimates, one per possible mismatch. Data are absent for the extremal locations  $x = 1$  and  $x = 25$ , since no value can be calculated by the NN model.

case of RNA duplexes in [19] (longer distances were not considered that case). We investigated antiparallel GA and AG pairs of mismatches also in sequences  $t_2$  and  $t_3$ , but found no anomalous behavior in those cases. This suggests that the nucleotide sequences between the two GA/AG pairs plays an important role in the overall stability of the duplex.

As a further proof of the outlying behavior of antiparallel GA/AG pairs we show in Figure 7 a plot of free energy penalties for tandem mismatches (neighboring double mismatches). These are again obtained from Equation (6) for different  $m$  and  $n$  mismatching nucleotides,

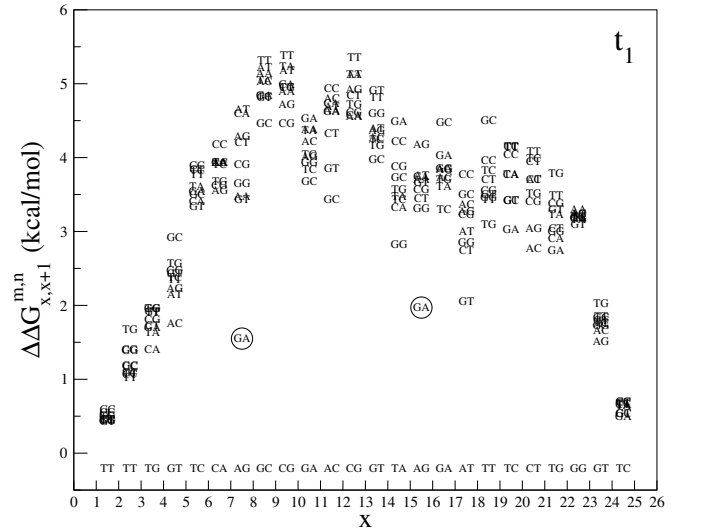


FIG. 7. The free energy penalty of tandem mismatches, from experiment with target  $t_1$ :  $\Delta\Delta G \left( \frac{xmny}{x'aby'} \right)$ , where  $x'$  and  $y'$  are complementary to  $x$  and  $y$  respectively.  $ab$  denoted above the x-axis are the fixed nucleotides in the target.  $mn$  is a tandem mismatch in the probe and the vertical position of these letters in the plot give the associated free energy penalty. Note the low free energy penalty for  $\frac{5'-GA-3'}{3'-AG-5'}$  mismatches (encircled).

where in the case of tandem mismatches,  $\Delta x$  is equal to 1. On each location of the sequence our data set contains nine different types of tandem mismatch. A clear boundary effect is noticeable, but when looking at the bulk data points tandem mismatch of the type GA/AG are again outlying, they appear to be particularly stable with a free energy penalty  $\sim 2$  kcal/mol below average.

#### IV. DISCUSSION AND CONCLUSION

In this article, we have analyzed DNA hybridization reactions in microarrays and quantified free energy penalties of single and double mismatches. We have shown that the experimental data are very precise and reproducible. The microarray data follow an equilibrium isotherm over a range of four orders of magnitude in the fluorescence intensities and allow the extraction of accurate thermodynamic parameters. First, the analysis provides a database with a large number of NN parameters for isolated mismatches. These parameters correlate well with those reported in the literature from hybridization experiments in solution. Second, the experiments contain systematic measurements of hybridization with two mismatches, which allowed us to probe the validity limit of the NN approximation. We showed that when two mismatches are separated by a distance of  $\geq 5$  nt their effect is additive, allowing a standard approach with the NN model. However, for shorter distances, the additivity is no longer valid and we found that duplexes with neighboring mismatches are more stable than expected from additivity. This interaction was shown to decay exponentially as a function of the distance between mismatches. Further, we investigated the behavior of mismatches close to the helix edges, and showed that their free energy penalty is reduced up to 80% when compared to the bulk behavior. The boundary effect was observable up to 4 nt from the helix edge. Finally, we also found some thermodynamic outliers, sequences involving two antiparallel GA mismatches, in which the mismatch interaction appears to persist beyond 5 nt. These outliers were not related to experimental error indicating a signature of some structural conformational change of a double helix containing these mismatch pairs.

Overall, the analysis of the microarray data reported in this article provides new quantitative insights on the DNA hybridization parameters, on the NN model and its present limitations. Our study is in line with a number of

recent articles, which have been dedicated to the investigations of fundamental physico-chemical properties of DNA arrays [22–31]. Due to the relevance of hybridization in many technologies, going from PCR [1] to recent developments in biosensors, e.g. [32], a good thermodynamic model is also important from the application point of view. A precise quantification of interaction free energies involved in the hybridization will help to increase the accuracy of microarrays and other hybridization-based technologies, so that these devices could realize their full potential, for instance, for clinical applications [33]. For these applications, an increase in specificity and sensitivity is very important and can be achieved through better understanding of fundamental properties of hybridization in these devices.

There has been considerable attention in recent years [9, 22, 24–34] in understanding the fundamentals of hybridization in DNA microarrays and its impact in data analysis. Here, we have shown that microarrays are a reliable and high-throughput tool to gain insight on DNA hybridization thermodynamics. The same method could be used to screen other types of defects, as bulges. Indeed, it was recently used for understanding loop conformations [22].

#### V. SUPPLEMENTARY DATA

Supplementary Data available in Appendix.

#### VI. ACKNOWLEDGEMENTS

We thank Karen Hollanders for expert technical assistance. We acknowledge financial support from Research Foundation-Flanders (FWO) Grant No. G.0311.08, KULeuven Grant No. STRT1/09/042 and VITO Grant ZL39010200-401.

Conflict of interest statement: *None declared.*

- 
- [1] Alberts, B., Johnson, A., Lewis, J., Raff, M., Roberts, K. and Walter, P. (2002) *Molecular Biology of the Cell*. Garland Science, New York.
  - [2] Breslauer, K.J., Frank, R., Blöcker, H. and Marky, L.A. (1986) Predicting DNA duplex stability from the base sequence. *Proc. Nat. Acad. Sci. USA*, **83**, 3746–3750.
  - [3] SantaLucia, J. Jr. (1998) A unified view of polymer, dumbbell, and oligonucleotide DNA nearest-neighbor thermodynamics. *Proc. Nat. Acad. Sci. USA*, **95**, 1460–1465.
  - [4] Sambriski, E.J., Schwartz, D.C. and de Pablo, J.J. (2009) A Mesoscale Model of DNA and Its Renaturation. *Biophys. J.*, **96**, 1675–1690.
  - [5] Bloomfield, V.A., Crothers, D.M. and Tinoco, I. Jr. (2000) *Nucleic Acids Structures, Properties and Functions*. University Science Books, Mill Valley.
  - [6] Mathews, D.H., Disney, M.D., Childs, J.L., Schroeder, S.J., Zuker, M. and Turner, D.H. (2004) Incorporating chemical modification constraints into a dynamic programming algorithm for prediction of RNA secondary structure. *Proc. Nat. Acad. Sci. USA*, **101**, 7287–7292.
  - [7] Andronescu, M., Condon, A., Hoos, H.H., Mathews, D.H. and Murphy, K.P. (2010) Computational approaches for RNA energy parameter estimation. *RNA*, **16**, 2304–2318.
  - [8] SantaLucia, J. Jr. and Hicks, D. (2004) The thermodynamics of DNA structural motifs. *Annu. Rev. Biophys. Biomol. Struct.*, **33**, 415–440.
  - [9] Hooyberghs, J., Van Hummelen, P. and Carlon, E. (2009) The effects of mismatches on hybridization in DNA microarrays: determination of nearest neighbor parameters. *Nucleic Acids Res.*, **37**, e53.

- [10] Atkinson, A.C. and Donev, A.N. (1992) *Optimum Experimental Designs*. Clarendon Press, Oxford.
- [11] Hooyberghs, J., Baiesi, M., Ferrantini, A. and Carlon, E. (2010) Breakdown of thermodynamic equilibrium for DNA hybridization in microarrays. *Phys. Rev. E*, **81**, 012901.
- [12] Gray, D.M. (1997) Derivation of nearest-neighbor properties from data on nucleic acid oligomers. I. Simple sets of independent sequences and the influence of absent nearest neighbors. *Biopoly.*, **42**, 783–793.
- [13] Walter, J.-C., Kroll, K.M., Hooyberghs, J. and Carlon, E. (2011) Nonequilibrium Effects in DNA Microarrays: A Multiplatform Study. *J. Phys. Chem. B*, **115**, 6732–6739.
- [14] Li, Y., Zon, G. and Wilson, W.D. (1991) Thermodynamics of DNA duplexes with adjacent G.cntdot.A mismatches. *Biochem.*, **30**, 7566–7572.
- [15] Li, Y., Zon, G. and Wilson, W.D. (1991) NMR and molecular modeling evidence for a G.A mismatch base pair in a purine-rich DNA duplex. *Proc. Nat. Acad. Sci. USA*, **88**, 26–30.
- [16] SantaLucia, J. Jr. and Turner, D.H. (1993) Structure of (rGGCGAGCC)<sub>2</sub> in solution from NMR and restrained molecular dynamics. *Biochem.*, **32**, 12612–12623.
- [17] Lane, A., Ebel, S. and Brown, T. (1994) Properties of multiple G · A mismatches in stable oligonucleotide duplexes. *Eur. J. Biochem.*, **220**, 717–727.
- [18] Ebel, S., Brown, T. and Lane, A.N. (1994) Thermodynamic stability and solution conformation of tandem G · A mismatches in RNA and RNA · DNA hybrid duplexes. *Eur. J. Biochem.*, **220**, 703–715.
- [19] Morse, S.E. and Draper, D.E. (1995) Purine-purine mismatches in RNA helices: evidence for protonated G.A pairs and next-nearest neighbor effects. *Nucleic Acids Res.*, **23**, 302–306.
- [20] Seela, F. and Budow, S. (2008) Mismatch formation in solution and on DNA microarrays: how modified nucleosides can overcome shortcomings of imperfect hybridization caused by oligonucleotide composition and base pairing. *Mol. BioSyst.*, **4**, 232–245.
- [21] Chang, C.Y.(J.) and Stellwagen, N.C. (2011) Tandem GA Residues on Opposite Sides of the Loop in Molecular Beacon-like DNA Hairpins Compact the Loop and Increase Hairpin Stability. *Biochem.*, **50**, 9148–9157.
- [22] Trapp, C., Schenkelberger, M. and Ott, A. (2011) Stability of double-stranded oligonucleotide DNA with a bulged loop: a microarray study. *BMC Biophys.*, **4**, 20.
- [23] Golovkin, M.V., Matveeva, O.V. and Nechipurenko, Iu.D. (2009) Properties of hybridization isotherms upon binding of ligands on microchips. *Biofizika*, **54**, 820–823.
- [24] Pozhitkov, A.E., Boube, I., Brouwer, M.H. and Noble, P.A. (2010) Beyond Affymetrix arrays: expanding the set of known hybridization isotherms and observing pre-wash signal intensities. *Nucleic Acids Res.*, **38**, e28.
- [25] Irving, D., Gong, P. and Levicky, R. (2010) DNA Surface Hybridization: Comparison of Theory and Experiment. *J. Phys. Chem. B*, **114**, 7631–7640.
- [26] Fuchs, J., Fiche, J.B., Buhot, A., Calemczuk, R. and Livache, T. (2010) Salt Concentration Effects on Equilibrium Melting Curves from DNA Microarrays. *Biophys. J.*, **99**, 1886–1895.
- [27] Burden, C.J. and Binder, H. (2010) Physico-chemical modelling of target depletion during hybridization on oligonucleotide microarrays. *Phys. Biol.*, **7**, 016004.
- [28] Qamhie, K., Wong, K.-Y., Lynch, G.C. and Pettitt, B.M. (2009) The melting mechanism of DNA tethered to a surface. *Int. J. Numer. Anal. Model.*, **6**, 474–488.
- [29] Gharaibeh, R.Z., Fodor, A.A. and Gibas, C.J. (2010) Accurate estimates of microarray target concentration from a simple sequence-independent Langmuir model. *PLoS One*, **5**, e14464.
- [30] Lee, C.-Y., Harbers, G.M., Grainger, D.W., Gamble, L.J. and Castner, D.G. (2007) Fluorescence, XPS, and TOF-SIMS surface chemical state image analysis of DNA microarrays. *J. Am. Chem. Soc.*, **129**, 9429–9438.
- [31] Binder, H., Preibisch, S. and Kirsten, T. (2005) Base pair interactions and hybridization isotherms of matched and mismatched oligonucleotide probes on microarrays. *Langmuir*, **21**, 9287–9302.
- [32] van Grinsven, B., Vanden Bon, N., Grieten, L., Murib, M., Janssens, S.D., Haenen, K., Schneider, E., Ingebrandt, S., Schöning, M.J., Vermeeren, V., Ameloot, M., Michiels, L., Thoelen, R., De Ceuninck, W. and Wagner, P. (2011) Rapid assessment of the stability of DNA duplexes by impedimetric real-time monitoring of chemically induced denaturation. *Lab Chip*, **11**, 1656–1663.
- [33] Hooyberghs, J. and Carlon, E. (2010) Hybridisation thermodynamic parameters allow accurate detection of point mutations with DNA microarrays. *Biosens. Bioelectron.*, **26**, 1692–1695.
- [34] Shanahan, H.P., Memon, F.N., Upton, G.J.G. and Harrison, A.P. (2012) Normalized Affymetrix expression data are biased by G-quadruplex formation. *Nucleic Acids Res.*, **40**, 3307–3315.



## SUPPLEMENTARY DATA

### Appendix A: Nearest neighbor model and linear regression

According to the nearest-neighbor model, the total hybridization free energy of a target to a probe can be expressed as a sum of the dinucleotide parameters  $\Delta G_\alpha$  accounting for hydrogen bonding and stacking interactions. The index  $\alpha$  covers all possible dinucleotide parameters. Some examples are:

$$\begin{aligned} \Delta G \left( \begin{array}{c} 5' - AT - 3' \\ 3' - TA - 5' \end{array} \right), \\ \Delta G \left( \begin{array}{c} 5' - AC - 3' \\ 3' - TG - 5' \end{array} \right), \\ \Delta G \left( \begin{array}{c} 5' - A\bar{A} - 3' \\ 3' - T\bar{A} - 5' \end{array} \right) \end{aligned} \quad (A1)$$

where the underlined nucleotides indicate mismatches. In total there are 10 perfect match parameters (taking into account symmetries) and 48 parameters in the case of a single mismatch. These dinucleotide parameters are known not to be unique, see e.g. [1].

Thermodynamics predicts that the intensity measured from a spot  $I_i$  is given by:

$$I_i = I_0 + Ace^{-\Delta G_i/RT} \quad (A2)$$

where  $\Delta G_i$  is the total hybridization free energy between a target and a probe,  $A$  is a parameter which sets the intensity scale,  $c$  the target concentration,  $R$  the gas constant and  $T$  the temperature.  $I_0$  is the aspecific signal that can be considered as background. In this paper the stability of duplexes was always compared to that of the perfect match, i.e.

$$y_i \equiv \ln I_i - \ln I_{PM} = -\frac{\Delta G_i - \Delta G_{PM}}{RT} \quad (A3)$$

which defines the free energy penalty of probe  $i$  with respect to the perfectly matching probe. This penalty can be expressed as a sum of nearest-neighbor dinucleotide parameters:

$$y_i = \sum_{\alpha=1}^{58} X_{i\alpha} \frac{\Delta G_\alpha}{RT} \quad (A4)$$

where  $X_{i\alpha}$  is the frequency matrix, which counts the number of times a given dinucleotide term contributes to  $y_i$ . As an example, for an isolated mismatch of type

GA we have:

$$\begin{aligned} \Delta G_i \left( \begin{array}{c} \dots G\bar{A}T \dots \\ \dots C\bar{G}A \dots \end{array} \right) - \Delta G_{PM} \left( \begin{array}{c} \dots GCT \dots \\ \dots CGA \dots \end{array} \right) = \\ \Delta G \left( \begin{array}{c} G\bar{A} \\ C\bar{G} \end{array} \right) + \Delta G \left( \begin{array}{c} A\bar{G} \\ T\bar{A} \end{array} \right) \\ - \Delta G \left( \begin{array}{c} GC \\ CG \end{array} \right) - \Delta G \left( \begin{array}{c} CT \\ GA \end{array} \right) \\ \equiv \Delta \Delta G \left( \begin{array}{c} G\bar{A}T \\ C\bar{G}A \end{array} \right) \end{aligned} \quad (A5)$$

For notational convenience we used, by symmetry, the equality of  $\Delta G \left( \begin{array}{c} A\bar{T} \\ \bar{G}A \end{array} \right) = \Delta G \left( \begin{array}{c} A\bar{G} \\ T\bar{A} \end{array} \right)$  to have the mismatch on the right hand side of the dinucleotide. For any given  $i$ , the matrix elements  $X_{i\alpha}$  are all zero except for the four dinucleotide terms of Equation (A5) which contribute by +1 for the two dinucleotides with mismatches and -1 for the two perfect matching dinucleotides. Equation (A4) defines a multiple linear regression, from which the 58 dinucleotide parameters can be fitted to match all the observed free energy penalties of mismatches. Note that it defines the dinucleotide parameters not in a unique way, e.g. the following transformation

$$\Delta G \left( \begin{array}{c} x\bar{A} \\ x'\bar{G} \end{array} \right) \rightarrow \Delta G \left( \begin{array}{c} x\bar{A} \\ x'\bar{G} \end{array} \right) + \varepsilon \quad (A6)$$

$$\Delta G \left( \begin{array}{c} x\bar{G} \\ x'\bar{A} \end{array} \right) \rightarrow \Delta G \left( \begin{array}{c} x\bar{G} \\ x'\bar{A} \end{array} \right) - \varepsilon \quad (A7)$$

in which the same constant  $\varepsilon$  is added and subtracted to different dinucleotide parameters, leaves Equation (A5) invariant. The triplet parameters, such as defined in the last line of Equation (A5) are however unique as expected, since they are directly physically accessible.

### Appendix B: Target sequence selection with Optimal design

As discussed above, the dinucleotide parameters can be obtained from a linear fit from  $N$  independent experimental measurements. Such an approach always contains some uncertainties. These uncertainties can be lowered if one takes  $N$  large. In our specific case  $N$  equals the number of spots on the microarrays, and can be increased by combining data from more arrays (see main paper for experimental setup). Further, for a given fixed value of  $N$  one can use some optimization criterion to select the best  $N$  measurements which minimize the uncertainties on fitted parameters. In our case this comes down to the selection of a target sequence with good statistical properties. The theory of *Optimal Design* establishes some criteria for this purpose and we briefly discuss this theory here.

Before entering into the details of the optimization followed in the microarray experiment we discuss a one dimensional example, which illustrates the optimization

method. Let us take the example of a simple linear regression with an intersect set to zero (corresponding to a one-dimensional system):

$$y_i = \beta x_i, \quad (\text{B1})$$

where  $\beta$  is the unknown of the problem,  $x_i$  and  $y_i$  are respectively the input and output of the experiment  $i$  and can take any real value. The parameter  $\beta$  can be obtained by the least square method :

$$\beta = \frac{\sum (x_i - \bar{x})(y_i - \bar{y})}{\sum (x_i - \bar{x})^2}, \quad (\text{B2})$$

where the symbol  $\bar{\cdot}$  means the average over the  $N$  elements. The error on  $\beta$  is given by :

$$\Delta\beta \underset{N \gg 1}{=} \frac{S}{N} \sqrt{\frac{1}{\sum (x_i - \bar{x})^2}}, \quad (\text{B3})$$

where  $S$  is the cost function of the system. Equation (B3) implies that the error can be decreased by enlarging the sampled points ( $N$ ) or, for  $N$  fixed, by increasing the variance of the variable  $x_i$ . The latter criterion can be used in the design of the experiment by performing measurements  $y_i$  for a well spread set of points  $x_i$ . Indeed, it is intuitively clear that when  $x_i$  are very close to each other (small variance) one has a large uncertainty on the estimate of the slope  $\beta$ . In what follows we discuss about optimal design criteria in higher dimensions, which roughly correspond to the idea of the maximization of the variance in the previous one-dimensional example.

We define first the so-called *information matrix*  $M = X^T X$ , where  $X$  is the frequency matrix defined in Equation (A4) and where  $X^T$  denotes its transpose. In terms of matrix elements:

$$M_{\alpha\beta} = \sum_{i=1}^N X_{i\alpha} X_{i\beta} \quad (\text{B4})$$

which is thus in our case a square symmetric matrix of dimension  $58 \times 58$ .

The information about the quality of the experimental design is encoded in  $M$  and in our case is defined by the sequence of the target oligo in the experiment (see main paper for experimental setup). The three most used criteria in optimal design are the A-, D- and E-optimality. A-optimality corresponds to minimizing the trace of  $M^{-1}$ , D-optimality corresponds to minimizing the determinant of  $M^{-1}$  and E-optimality corresponds to maximizing the lowest eigenvalue of  $M$ . Roughly speaking, these strategies amounts to maximize the information encoded in  $M$  [2]. We note that in the linear problem of Equation (A4) the information matrix has a minimum of 7 null eigenvalues (see the supplementary material of Ref. [3] for a detailed explanation). These come from unavoidable degeneracies of the problem, or equivalently from the fact that the dinucleotide parameters are not unique (see e.g.

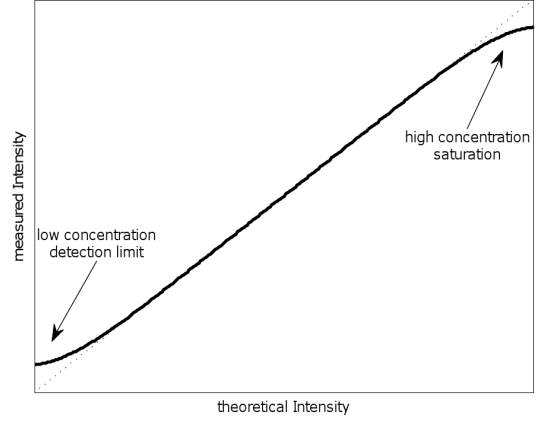


FIG. 8. Sketch to show non-linear behaviour due to detection limit on low end and saturation on high end.

Equations (A6) and (A7)). Having some zero eigenvalues, the information matrix  $M$  is not invertible, therefore we are working with pseudo-inverse which is obtained from the singular value decomposition of  $M$ .

The three target sequences,  $t_1, t_2$  and  $t_3$ , which were used for the experiments and which are mentioned in table 1 of the main article were selected as follows. We collected a set of candidate targets by scanning over a piece of the human genome and taking subsequences of length 25. The first criterion was to choose sequences with minimum, unavoidable, number of 7 zero eigenvalues in order to get the minimum number of degeneracies when solving the linear system to estimate the nearest-neighbor parameters, as discussed above. For  $t_1$ , we considered a subset of sequences with a minimum distance of 3 nucleotides from the border and a minimum distance of 3 nucleotides between 2 mismatches. For  $t_2$  and  $t_3$ , the minimal distance from the border is 4 nucleotides and the distance between 2 mismatches is at least 5 nucleotides. Therefore, the constraint on the subset to select  $t_1$  was weaker than  $t_2$  and  $t_3$ . Since the constraint for  $t_2$  and  $t_3$  is stronger than  $t_1$ , in this case, the number of equations in the linear system is lower and it is more difficult to find subsequences of length 25 which display the minimum number of 7 zero eigenvalues. For the same order of calculation, we managed to find 130 sequences for  $t_1$  and only a few sequences for  $t_2$  and  $t_3$ . For  $t_1$ , this set of candidates was subsequently ranked according to the three optimal design criteria A, D and E. Finally, the candidate targets which ended up as top-ranked on all three criteria were retained. Moreover, we checked the energy for the target to fold on itself. For the 3 targets, it takes a reasonable value.

### Appendix C: The linear regime

As a measurement device the microarray technology is faced with a detection limit in the low measurement regime and a saturation in the high end: see sketch in

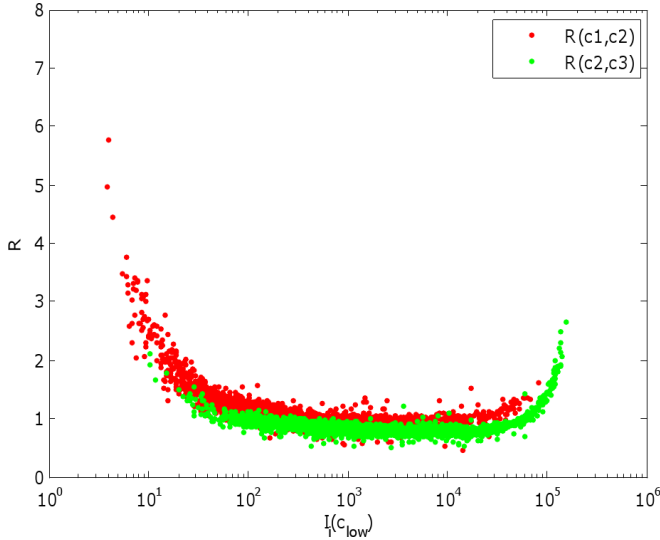


FIG. 9. Plot of  $R_i(c_n, c_{n+1})$ ,  $c_{n+1} > c_n$ , as a function of the Intensity  $I_i(c_n)$ . The used target concentrations are  $c_1 = 20pM$ ,  $c_2 = 100pM$ ,  $c_3 = 500pM$  of target  $t_2$ .

Figure 8. In our research we want to limit ourselves to measurements in the linear regime. To assess which data meet this requirement we combine experiments which are identical (identical target sequence, identical probe sets, identical hybridisation conditions) except for the concentration  $c_n$  of the target. If the data is in the linear regime we expect the intensity of a spot  $i$  of the experiment with target concentration  $c_n$  to be

$$I_i \propto c_n \exp(-\Delta G_i / RT). \quad (C1)$$

If we now combine two experiments, one with target concentration  $c_n$  and one with  $c_{n+1} > c_n$ , and define for each spot  $i$  the quantity  $R$  as

$$R_i(c_n, c_{n+1}) = \frac{I_i(c_n)}{I_i(c_{n+1})} \frac{c_{n+1}}{c_n} \quad (C2)$$

than we expect  $R$  to be equal to 1 when both intensities are in the linear regime. However for low  $c_n$  the spot intensity  $I_i(c_n)$  can be close to detection limit and consequently be higher than predicted by the theory of Equation (C1), or for high  $c_{n+1}$  the intensity  $I_i(c_{n+1})$  can be close to saturation and consequently lower than theoretically expected. In both cases  $R$  will be above one. The result of this analysis is shown in Figure 9

for the combinations ( $c_1 = 20pM, c_2 = 100pM$ ) and ( $c_2 = 100pM, c_3 = 500pM$ ) of target  $t_2$ . From this picture it is clear that for a large part of the intensity range  $R$  equals one and supports the linear regime. For the green dots, there is a deviation in the high intensity range due to the proximity of saturation of these spots in the  $500pM$  experiment. For the red dots a deviation is present due to proximity of the detection limit for these spots in the  $20pM$  data. This approach gives a criterion to assess the validity of the linear regime per spot and the possibility to make a correction for the non-linear behaviour close to saturation or detection limit.

#### Appendix D: Free energy additivity of mismatches

In the main article the additivity of free energy penalties of mismatches was shown when mismatches were separated by more than four nucleotides. For two examples, this was explicitly shown in Figure 5 of the main article. In this section we add some further examples of the additivity with similar plots. These are shown in Figure 10.

#### Appendix E: Self-consistency in free energy penalties estimation of triplet nucleotides

In the main article we present two different approaches that can be used to estimate free energy penalties of single mismatches in a triplet of nucleotides such as in Equation (3) of the main article. The first method, i.e. by linear fitting, produces a robust estimation provided that each of the 58 NN dinucleotide parameters are equally well-represented. This was achieved by the use of Optimal Design principle in designing the experiments. Another method is by taking the median of data points from ratios of intensities following Equations (4)-(6) of the main article. Figure 10 of this document shows six of these unique triplets in which the free energy penalties are indicated by the horizontal line from taking the median of each independent estimates. It is then imperative to see if these two methods are equivalent in providing the estimates. Figure 11 shows that the free energy penalties calculated from the two methods are well-correlated with Pearson correlation 0.966 (such as mentioned in the main article). This is indicating the equivalence of the two methods. This is also a proof that our experiments are self-consistent from the different perspective of these two approaches.

[1] Gray, D.M. (1997) Derivation of nearest-neighbor properties from data on nucleic acid oligomers. I. Simple sets of independent sequences and the influence of absent nearest neighbors. *Biopoly.*, **42**, 783–793.

[2] Atkinson, A.C. and Donev, A.N. (1992) *Optimum Experimental Designs*. Clarendon Press, Oxford.

[3] Hooyberghs, J., Van Hummelen, P. and Carlon, E. (1992) The effects of mismatches on hybridization in DNA microarrays: determination of nearest neighbor parameters. *Nucleic Acids Res.*, **37**, e53.

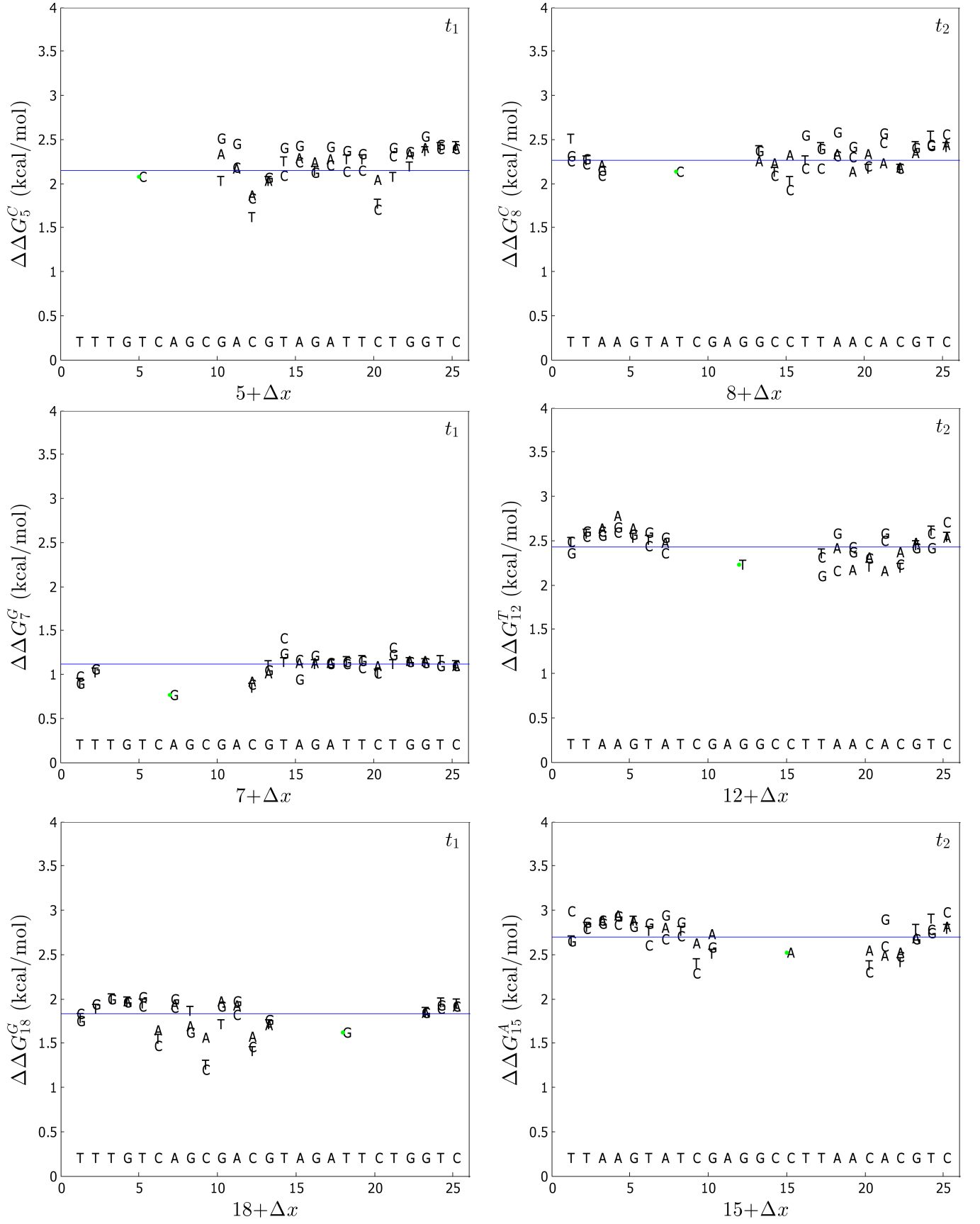


FIG. 10. A few examples of different focus mismatches showing additivity as  $|\Delta x| > 4$ . Similar to Figure 5 in the main paper, the target shown in top of the x-axis is in 3' to 5' orientation,  $t_1$  are on the left side,  $t_2$  are on the right side.

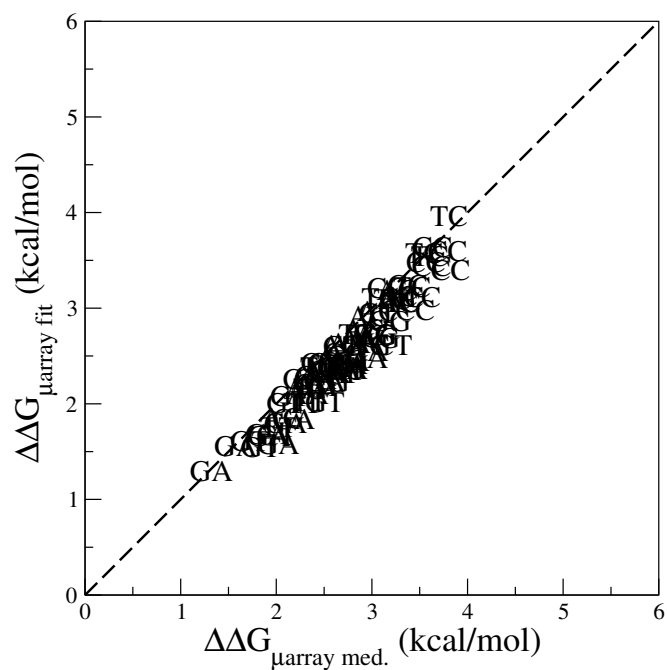


FIG. 11. Comparison of estimates of free energy penalties for isolated mismatches, obtained in two different ways: from the linear model fit and from the median of independent estimates. The two sets of data are strongly correlated (Pearson's correlation 0.966).